Cylindrical cavity expansion in Hoek-Brown rock

Analytical Solution with experimental validation through pressuremeter tests in marls and numerical modeling

Sami Hamdi[1] and *Steve Gruslin*[1]

[1]*GEOCONSEILS S.A., Department of Geotechnics and Engineering Geology, 4, rue Albert Simon, L-5315 Contern, Luxembourg*
Corresponding author: sami.hamdi@geoconseils.lu

ABSTRACT

The cylindrical cavity expansion problem is an important aspect of geotechnical engineering, with applications in tunneling, geothermal exploration, drilling activities, and underground construction. This study develops a closed-form analytical solution for the expansion of cylindrical cavities in rock masses modeled as elastic-plastic media using the Hoek-Brown (H-B) yield criterion. The solution uses the Lambert W function to express stress distributions, while strains are calculated based on a non-associated plastic flow rule. Key results include predictions for the yielding pressure, plastic zone extent, and stress profiles around the cavity.

To validate the analytical model, pressuremeter tests were conducted in marls, providing experimental data for comparison. Finite element analyses (FEA) were also performed using PLAXIS 2D, with the Hoek-Brown criterion implemented to ensure consistency. Calibration of the numerical model confirmed the accuracy of the simulations for the cavity expansion process.

A comparison of the analytical solution, experimental data, and numerical results shows good agreement, supporting the reliability of the proposed method. While some discrepancies are observed, particularly in the transition between elastic and plastic zones, the analytical approach offers a useful tool for predicting key parameters such as yielding pressure, stress distribution, and plastic zone extent. These results suggest that the analytical method can serve as an efficient alternative to numerical simulations in certain geotechnical applications, particularly when computational efficiency is desired. This study contributes to a deeper understanding of cavity expansion mechanics in rock masses and provides practical insights for the design and analysis of underground structures.

RESUME

Le problème de l'expansion de cavités cylindriques est crucial en ingénierie géotechnique, notamment pour le tunnelier, l'exploration géothermique, le forage et la construction souterraine. Cette étude propose une solution analytique pour l'expansion des cavités cylindriques dans des masses rocheuses modélisées comme des milieux élasto-plastiques selon le critère de Hoek-Brown. La solution utilise la fonction Lambert W pour exprimer les distributions de contraintes, tandis que les déformations sont calculées à l'aide d'une règle de flux plastique non associée. Les principaux résultats incluent la prédiction de la pression de rupture, l'étendue de la zone plastique et les profils de contraintes autour de la cavité.

Afin de valider le modèle, des essais de pressiomètre ont été réalisés dans des marnes, fournissant des données pour la comparaison. Des simulations par éléments finis (PLAXIS 2D) ont également été effectuées, intégrant le critère de Hoek-Brown. La calibration du modèle numérique a confirmé la précision des simulations.

Les comparaisons entre la solution analytique, les données expérimentales et les résultats numériques montrent une bonne cohérence, validant la méthode proposée. Bien que des divergences existent dans la transition entre zones élastiques et plastiques, l'approche analytique permet de prédire des paramètres clés comme la pression de rupture et la zone plastique. Cette méthode représente une alternative efficace aux simulations numériques, surtout lorsque l'efficacité de calcul est nécessaire, et offre des perspectives pour la conception des structures souterraines.

Keywords: Cylindrical cavity expansion, Lambert W function, Hoek-Brown, pressuremeter tests, marls, PLAXIS 2D, yielding pressure.

1. Introduction

Cavity expansion theory plays a fundamental role in geotechnical engineering for modeling stress and deformation around expanding voids. Initially developed for soils to study pile installation and bearing capacity (Vesic, 1972; Carter et al., 1986; Randolph et al., 1994), it has since been extended to rock mechanics for applications in tunneling, drilling, and underground construction.

In rock masses, the Hoek-Brown (H-B) failure criterion (Hoek & Brown, 1980) provides a realistic description of nonlinear strength behavior. However, few analytical cavity expansion solutions have been developed using this criterion due to its complexity. Carranza-Torres (1998) analyzed circular tunnels using a Tresca yield criterion, and Wang & Yin (2011) derived solutions for spherical cavities under Mohr-Coulomb and Hoek-Brown models, but no general closed-form solution for cylindrical expansion in H-B media has been widely adopted.

This study addresses that gap by proposing a closed-form analytical solution for cylindrical cavity expansion in Hoek-Brown media, incorporating a non-associated plastic flow rule. The solution is expressed using the Lambert W function and is validated through pressuremeter tests in marls and numerical simulations using PLAXIS 2D. The approach offers an efficient tool for evaluating yielding pressure, stress distribution, and plastic zone extent in rock engineering problems.

2. Analytical solution for cylindrical cavity expansion in Hoek-Brown rock

2.1. Hoek-Brown failure criterion

The Hoek-Brown failure criterion is widely accepted for rock masses and has been applied in a large number of projects around the world. Hoek and Brown (1980, 1988) introduced their failure criterion with a view to provide input data to analyses required for the design of underground excavations in hard rock. The criterion was derived from a combination of results of research on the brittle failure of intact rock conducted by Hoek and on model studies of jointed rock mass behaviour conducted by Brown. The criterion started from the properties of intact rock, incorporating factors to reduce these properties when considering characteristics of joints affecting the rock mass. Based essentially on the results of triaxial compression testing, the Hoek-Brown yield criterion can be expressed in terms of principal stresses using rock materials constants as follows:

$$\sigma_1 = \sigma_3 + \sigma_{ci}\left(m_b\frac{\sigma_3}{\sigma_{ci}} + s\right)^{\alpha} \tag{1}$$

where

- σ_1 and σ_3 are respectively the major and minor effective principal compressive stresses
- σ_{ci} is the unconfined compressive strength of the intact rock
- m_b is the reduced value of the material constant m_i
- m_i, α, and s are material constants which can be expressed as functions of the geotechnical strength index (*GSI*) and the disturbance factor (*D*) as follows:

$$m_b = m_i e^{\left(\frac{GSI-100}{28-14D}\right)} \tag{2a}$$

$$s = e^{\left(\frac{GSI-100}{9-3D}\right)} \tag{2b}$$

$$\alpha = \frac{1}{2} + \frac{1}{6}\left(e^{\frac{-GSI}{15}} - e^{\frac{-100}{15}}\right) \tag{2c}$$

It can be noted that s=1 for the case of intact rock and that the value of α does not differ much from 0,5, the value suggested for the intact rock.

The Geological Strength Index (GSI), introduced by Hoek (1994), Hoek et al. (1995), and Marinos et al. (2005) provides a measure of the rock mass, when combined with the intact rock properties, can be used for estimating the reduction in rock mass strength. The disturbance factor D depends upon the degree of disturbance to which the rock mass has been subjected as a result of the execution or breaking up process. The value of this parameter is based on existing damage due to blasting or disturbance. It varies from 0 for undisturbed in situ rock masses to 1 for very disturbed rock masses. Guidelines for the selection of D are discussed in a later section

2.2. Problem statement

The wall of an infinitely long cylindrical cavity with radius r_0 in a homogeneous infinite rock mass is subjected to an internal pressure P. The medium is initially isotropic and subjected to a hydrostatic stress σ_0. The problem geometry and boundary conditions are depicted in Fig. 1 where a cylindrical coordinate system is adopted. Because of axial symmetry, the problem is reduced to a plane strain problem that can be fully depicted using a single radial coordinate ‘r’.

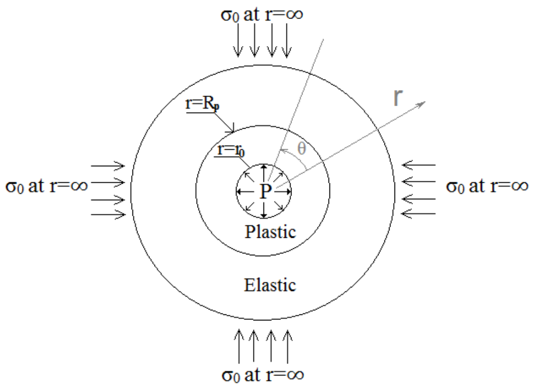

Figure 1. Cylindrical cavity expansion in rock mass.

The boundary conditions are expressed by the following equation:

$$\sigma_r(r=\infty)=\sigma_0 \quad (3a)$$

$$\sigma_r(r=r_0)=P \quad (3b)$$

Under the expansion of the cylindrical cavity, the major principal stress is the radial stress σ_r while the minor principal stress is the circumferential stress σ_θ. For the case of α =0,5, Eq. (1) becomes:

$$\sigma_r(r=r_0)=P \quad (4)$$

The equilibrium equation for this problem in terms of radial and circumferential stresses can be expressed as follows:

$$\frac{\partial\sigma_r}{\partial r}+\frac{\sigma_r-\sigma_\theta}{r}=0 \quad (5)$$

2.3. Analytical expression of yield pressure

An infinite homogeneous and isotropic elastic rock medium is considered to assess the yielding pressure P_{Yield} defined as the internal pressure indexing the onset of plasticity within the medium. The elastic equilibrium conditions of the medium in the elastic domain subjected to an internal pressure P is given in terms of stresses by the following equations:

$$\sigma_r=\sigma_0+(P-\sigma_0).\left(\frac{r_0}{r}\right)^2 \quad (6a)$$

$$\sigma_\theta=\sigma_0-(P-\sigma_0).\left(\frac{r_0}{r}\right)^2 \quad (6b)$$

It can be noted that the σ_r and σ_θ profiles are remarkably independent from the elastic parameters (Young's modulus E, Poisson's ratio ν). The yield pressure can be expressed by substituting Eq. (6) into Eq. (1):

$$P_{Yield}=\sigma_0+\frac{\sigma_{ci}}{8}\left(-m_b+\sqrt{m_b^2+16s+16m_b\frac{\sigma_0}{\sigma_{ci}}}\right) \quad (7)$$

It can also be noted that the yield pressure is independent from the radius of the cavity and from any assumed elastic parameters provided the medium is initially homogeneous and isotropic.

2.4. Stresses analysis

The circumferential stress can be expressed as a function of radial stress using Eq. (1):

$$\sigma_\theta=\sigma_r+\frac{\sigma_{ci}}{2}\left(m_b-\sqrt{m_b^2+4s+4m_b\frac{\sigma_r}{\sigma_{ci}}}\right) \quad (8)$$

The partial differential Eq. (5) can be bailed down in terms of σ_r to the following expression:

$$\frac{\partial\sigma_r}{\partial r}-\frac{\sigma_{ci}}{2.r}\left(m_b-\sqrt{m_b^2+4s+4m_b\frac{\sigma_r}{\sigma_{ci}}}\right)=0 \quad (9)$$

The solution of the above partial differential equation satisfying the boundary conditions Eq. (3) can be expressed as function the radial distance:

$$\sigma_r(r)=-\frac{\sigma_{ci}}{4m_b}\left(m_b^2+4s-m_b^2\{1+\omega(A)\}^2\right) \quad (10a)$$

$$A=Ln\left(\frac{1}{m_b}\right)-\left(C1+1+Ln\left(\frac{r}{r_0}\right)\right) \quad (10b)$$

The Wright omega function ω(z) as introduced by Calmet et al. (2002), is a function of a complex variable z and is defined using the Lambert W function:

$$\omega(z)=W_{k(z)}(e^z) \quad (11a)$$

where the branch index k=k(z) is given by

$$k(z)=\left\lceil\frac{Im(z)-\pi}{2\pi}\right\rceil \quad (11b)$$

Here, $W_k(z)$ denotes the k-th branch of the Lambert W function, which satisfies (Corless et al. 1996):

$$W_k(z).e^{W_k(z)}=z \quad (12a)$$

The W, the Lambert function, has an infinite number of branches, denoted W_k ($k \in \mathbb{Z}$).

The ceiling function $\lceil X\rceil$ selects the correct branch k so that ω(z) is a well-defined, single-valued function across the complex plane. This ensures ω(z) uniquely solves:

$$\omega(z)+ln(\omega(z))=z \quad (12b)$$

For real values of z: Im(z) = 0, the index k=0 since $\lceil(\mathrm{Im}(z)-\pi)/2\pi\rceil=\lceil-1/2\rceil=0$, and thus:

$$\omega(z)=W_0(e^z) \quad (12d)$$

The Wright Omega function is differentiable and satisfies the following equation:

$$\frac{d\omega(z)}{dz} = \frac{\omega(z)}{1+\omega(z)} \tag{12-c}$$

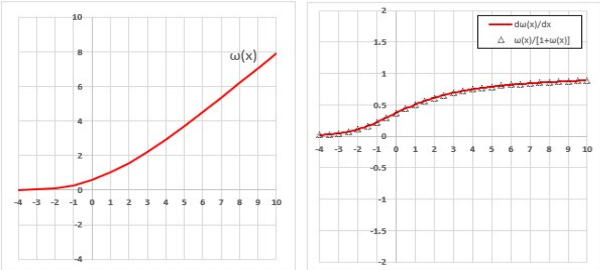

Figure 2. Wright Omega function.

C1 is a constant that depends upon the boundary conditions. When applying an internal pressure equal to P, C1 can be expressed as follows:

$$C1 = -Ln(-m_b + C2) - \frac{C2}{m_b} \tag{13a}$$

$$C2 = \sqrt{m_b^2 + 4.s + P.\frac{4m_b}{\sigma_{ci}}} \tag{13b}$$

The circumferential stress σ_θ in the plastic zone can be deduced based on Eq. (8).

The elastic-plastic interface r_p can be determined by explicitly solving the following equation:

$$\sigma_r(r_p) = P_{Yield} \tag{14}$$

where P_{Yield} is given by Eq. (7)

Finally, the plastic front r_p can be expressed as a function of the initial radius of the cavity r_0 by the following expression:

$$r_p = \frac{\sigma_{ci}.(m_b + C3).e^{-C1-\frac{C3}{m_b}}}{4.(m_b.P_{Yield} + s.\sigma_{ci})} r_0 \tag{15a}$$

$$C3 = \sqrt{m_b^2 + P_{Yield}.\frac{4m_b}{\sigma_{ci}} + 4.s} \tag{15b}$$

2.5. Displacement analysis

The radial and circumferential strains are expressed by the following formula:

$$\varepsilon_r = -\frac{\partial u_r}{\partial r} \tag{16a}$$

$$\varepsilon_\theta = -\frac{u_r}{r} \tag{16b}$$

where u_r is the radial displacement

Based on the classical theory of plasticity, the total strains are subdivided into their elastic and plastic components:

$$\varepsilon_r = \varepsilon_r^e + \varepsilon_r^p \tag{17a}$$

$$\varepsilon_\theta = \varepsilon_\theta^e + \varepsilon_\theta^p \tag{17b}$$

Elastic strains can be expressed by the following equation:

$$\varepsilon_r^e = \frac{1-\nu^2}{E}\left((\sigma_r - \sigma_0) - \frac{\nu}{1-\nu}(\sigma_\theta - \sigma_0)\right) \tag{18a}$$

$$\varepsilon_\theta^e = \frac{1-\nu^2}{E}\left(-\frac{\nu}{1-\nu}(\sigma_r - \sigma_0) + (\sigma_\theta - \sigma_0)\right) \tag{18b}$$

where E and ν are respectively the Young's modulus and the Poisson's ratio.

In order to evaluate displacements within the plastic zone, a plastic flow rule needs to be assumed. Adopting a non-associated flow rule, we obtain the following relationships between plastic strains, assuming that ε_z=0:

$$\varepsilon_r^p + \beta.\Delta\varepsilon_\theta^p = 0 \tag{19a}$$

$$\beta = \frac{1-sin(\psi)}{1+sin(\psi)} \tag{19b}$$

where ψ is the dilatancy angle.

Substituting equations Eqs. (16), (18), and (19) into Eq. (17), we obtain the following partial differential equation describing the radial displacement:

$$\frac{\partial u_r}{\partial r} + \beta\frac{u_r}{r} = g(r) \tag{20}$$

where:

$$g(r) = -\frac{1+\nu}{E}\left(C4(\sigma_r - \sigma_0) + C5(\sigma_\theta - \sigma_0)\right) \tag{21a}$$

$$C4 = 1 - \nu - \beta\nu \tag{21b}$$

$$C5 = \beta - \beta\nu - \nu \tag{21c}$$

Finally, the radial displacement can be expressed by the following equation:

$$u_r(r) = r^{-\beta}\left(r_p^\beta.u_{rp} + \int_{r_p}^{r} x^\beta.g(x)dx\right) \tag{22}$$

where, r_p is the plastic front position given by Eq. (15) while u_{rp} is the radial displacement at plastic front and is expressed by the following expression:

$$u_{rp} = \frac{1}{2G}(P_{Yield} - \sigma_0)r_p \tag{23}$$

3. Numerical validation

To validate the analytical solution for the expansion of a cylindrical cavity in a Hoek–Brown material (see Section 2), a comparison is conducted with numerical modeling using PLAXIS under axisymmetric conditions. The analysis considers different rock types, particularly varying uniaxial compressive strengths (cf. Table 1). The comparison focuses on key mechanical responses, including the stress field, the extent of the plastic zone, and radial displacement. This approach ensures a comprehensive assessment of the analytical solution's accuracy in capturing the mechanical behavior of the rock mass under cavity expansion.

Table 1. Basic Hoek-Brown parameters

	Case 1	Case 2	Case 3
σ_{ci} (MPa)	20	40	60
m_i (-)	7	7	7
GSI (-)	50	50	50
D (-)	0,2	0,2	0,2

Figures 3 to 5 show the comparison between analytical and numerical results for radial and circumferential stresses, under 1 MPa pressure and an initial cavity radius of 33 mm. Three cases are studied, with uniaxial compressive strengths of 20 MPa, 40 MPa, and 60 MPa (cf. Table 1). All other Hoek–Brown parameters remain unchanged.

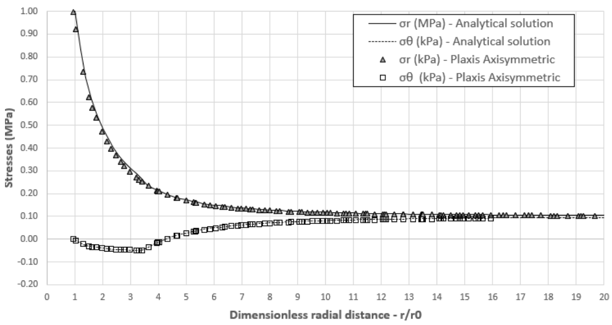

Figure 3. Radial stress comparison for a uniaxial compressive strength of 20 MPa (Case 1, Table 1).

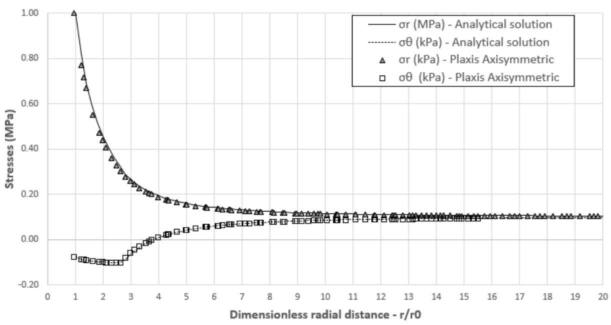

Figure 4. Radial stress comparison for a uniaxial compressive strength of 40 MPa (Case 2, Table 1).

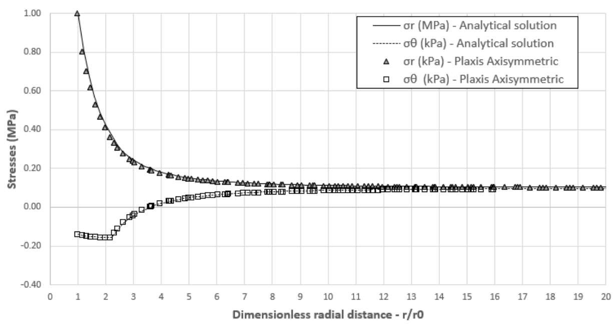

Figure 5. Radial stress comparison for a uniaxial compressive strength of 60 MPa (Case 3, Table 1).

Figure 6 shows the evolution of the plastic zone ('plastic front'), illustrated in red, calculated using finite element analysis (PLAXIS) for the three rock cases (see Table 1) and as a function of the applied pressure.

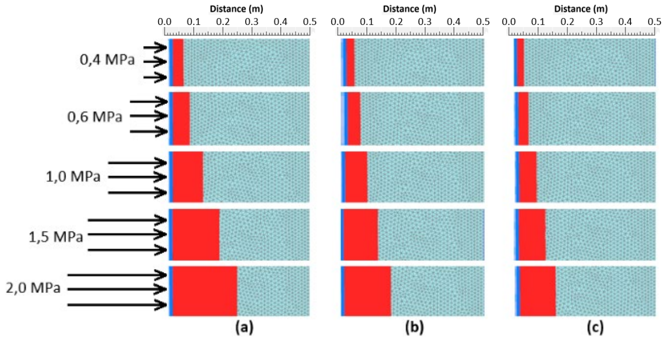

Figure 6. Evolution of the Plastic Zone ('Plastic Front') Calculated by Finite Element Analysis (PLAXIS) for Different Rock Cases and Applied Pressure: (a) Case 1, (b) Case 2 and (c) Case 3.

The graph in Figure 7 summarizes the results from Figure 5, comparing the analytical and finite element solutions in terms of the dimensionless plastic radius (R_P/R_0), with R_0 = 33 mm.

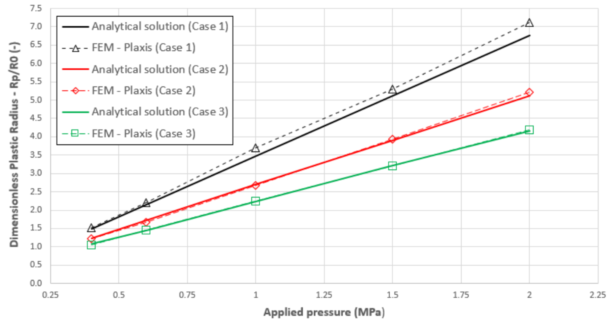

Figure 7. Comparison Between the Analytical Solution and Finite Element Calculation of the Plastic Front (Summary of Figure 6).

4. Comparison with pressuremeter tests

To validate the analytical solution for the expansion of a cylindrical cavity in a medium governed by the Hoek-Brown criterion, pressuremeter test results conducted in marls were analyzed. Marls, which are extensively distributed in southern Luxembourg and date back to the Triassic and Jurassic periods, exhibit a transitional behavior between soils and rigid rocks due to their mineralogical composition.

Their widespread occurrence allows for the acquisition of a large dataset, while their deformable rock-like characteristics make them particularly suitable for assessing the analytical solution. These factors collectively justify their selection as the reference material for validation.

For this analysis, a pressuremeter test in marl at 6 meters depth was considered, with an initial borehole radius of 33 mm. (cf. Figure 8 and Figure 9).

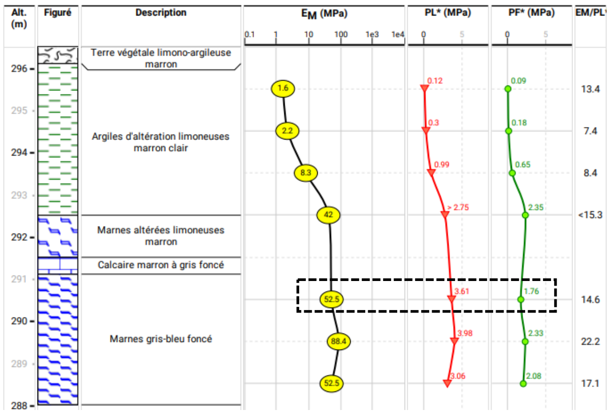

Figure 8. Lithology and Depth of the Test, and Interpreted Pressuremeter Parameters.

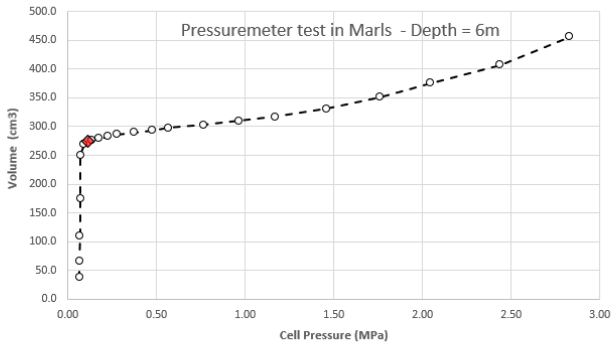

Figure 9. Evolution of the Central Cell Volume as a Function of Applied Pressure.

The following graph presents a comparison of pressuremeter test results, expressed in terms of radial displacement as a function of the applied pressure. The radial displacement was computed from the volume increment using the relation $\Delta r = \Delta V / (2\pi r_0)$, starting from the initial contact point between the probe and the borehole wall (highlighted in red in Figure 8), and was subsequently compared with the analytical solution.

To enhance the reliability of the interpretation, the pressuremeter test was numerically simulated using PLAXIS to calibrate the Hoek-Brown parameters, with a specific focus on the Geological Strength Index (GSI).

The calibrated Hoek-Brown parameters for the marl rock mass were determined as: $\sigma ci = 25$ MPa, $mi = 7$, GSI = 40, and D = 0. These values were subsequently used in the analytical solution for further validation (cf. Figure 10).

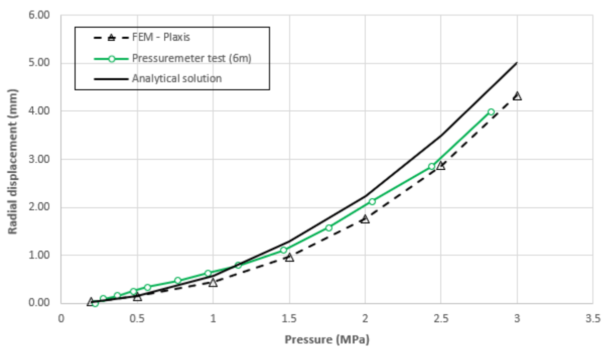

Figure 10. Comparison of Radial Displacement from the Pressuremeter Test and the Analytical Solution as a Function of Applied Pressure

This integrated approach, combining analytical solutions, numerical simulations, and experimental data, supports a reliable calibration method to identify Hoek-Brown parameters from pressuremeter tests. It demonstrates that in situ testing, when combined with appropriate calibration, can effectively provide accurate parameters and enhance the precision of geomechanical models for rock masses.

5. Conclusions

An analytical solution incorporating the Lambert W function was formulated to investigate the elastoplastic behavior of cylindrical cavity expansion in rock masses governed by the generalized Hoek-Brown (H-B) yield criterion. This solution provides explicit expressions for yielding pressure, plastic zone extent, stress distribution, and radial displacements, offering a rigorous framework for characterizing rock deformation under expansion loading.

To validate the proposed approach, numerical simulations were conducted using PLAXIS across various rock types. The results exhibited strong agreement between analytical predictions and numerical outcomes, particularly in terms of stress distribution, plastic zone development, and radial displacement profiles, reinforcing the robustness of the model.

Further verification was performed through comparison with pressuremeter test data, demonstrating a satisfactory level of consistency between analytical and experimental results. As part of ongoing research, additional comparisons will be carried out using an expanded dataset of pressuremeter tests on weak to low-strength rock formations. The overarching objective of this study is to establish a robust analytical calibration methodology for deriving Hoek-Brown parameters directly from pressuremeter test data, thereby improving the accuracy and applicability of geomechanical modeling in rock engineering.

6. References

- Journal articles

Carranza-Torres C (1998) Self-similarity analysis of the elasto-plastic response of underground openings in rock and effects of practical variables.Ph.D. Thesis, University of Minnesota.

Carter JP, Booker JR, Yeung SK (1986) Cavity expansion in cohesive frictional soils. Géotechnique 36: 345-358.

Dittes M, Labuz JF (2002) Field and Laboratory Testing of St. Peter Sandstone. Journal of Geotechnical and Geoenvironmental Engineering 128: 372-380.

Hoek E. (2007) Practical Rock Engineering. Available online: www.rocscience.com

Hoek E, Kaiser PK and Bawden.WF (1995) Support of underground excavations in hard rock. Rotterdam, Balkema.

Hoek, E. 1994.Strength of rock and rock masses, ISRM News J, 2(2): 4-16.

Hoek E, Brown ET (1988) The Hoek-Brown failure criterion - a 1988 update.Proc. 15th Canadian Rock Mech. Symp. (ed. J.C. Curran), 31-38. Toronto, Dept. Civil Engineering, University of Toronto.

Hoek E, Brown ET (1980) Empirical strength criterion for rock masses. J. Geotech. Engng Div., ASCE 106, 1013-1035.

Corless R.M. AND Jeffrey DJ (2002) The Wright ω function. In Calmet J, Benhamou B, Caprotti O, Henocque L, and Sorge V (Eds) Artificial Intelligence, Automated Reasoning, and Symbolic Computation: 76-89. Berlin: Sprinter. Doi: 10.1007/3-540-45470-5-10.

Marinos V., Marinos P., Hoek E. (2005) The geological Strength index: applications and limitations. Bulletin of Engineering Geology and the Environment 64: 55-65.

Randolph M.F., Dolwin J., Beck R. (1994) Design of driven piles in sand. Géotechnique 44: 427-448

Vesic A.C. (1972) Expansion of cavities in infinite soil mass. Journal of Soil Mechanics and Foundation Division, ASCE 98: 265-290.

Corless RM, Gonnet GH, Hare DEG, Jerey DJ, Knuth DE (1996) On the Lambert W Function. Advances in Computational Mathematics 5: 329-359

Wang S., Yin S. (2011) Strain-softening analysis of a spherical cavity. International journal for numerical and analytical methods in geomechanics 36: 182-202.

- Dissertations/Theses and e-version

HAMDI, S. "Pipe pile driving into rock", PhD dissertation, UCLouvain Belgium, 2016. [online] Available at: https://dial.uclouvain.be/pr/boreal/object/boreal:172501, accessed: 22/January/2016.

Acknowledgements

The authors are grateful for the financial support provided by the Walloon Region, Belgium. The project presented in this article is supported by Agreement Number 1250394.